

Design Strategies of Transmission Trunks across Normal Fault-- A Case Study of Shanchiao Fault

Sheng-Shin Chu, Chin-Ling Huang and Kai-Ping Chang

ABSTRACT

According to the studies about active faults in metropolitan Taipei area, it has been indicated that Shanchiao Fault at the western rim of Taipei Basin is a highly active normal fault. Slip of the fault can cause deformation of shallower soil layers and lead to the destruction of infrastructures, residential building foundations and utility lines like transmission trunks near or across the influenced area.

Data on geological drilling and dating have been used to determine that a growth fault exists in the Shanchiao Fault. In an experiment, a sandbox model was built using noncohesive sandy soil to simulate the existence of a growth fault in the Shanchiao Fault and forecast the effect of the growth fault on shear-band development and ground differential deformation. The experimental results indicated that when a normal fault contains a growth fault at the offset of the base rock, the shear band develops upward beside the weak side of the shear band of the original-topped soil layer, and surfaces considerably faster than that of the single-topped layer. The offset ratio required is approximately one-third that of the single-cover soil layer.

The finite element method (FEM), finite difference method (FDM), and discrete element method (DEM) are usually used to analyze the fault deformation. However, when the normal fault is simulated, the new overlay was deposited after the fault slip; the finite element method (FEM) of the continuum is hard for normal fault analysis. In former study, a numerical simulation of the sandbox experiment was conducted using a discrete element method program, PFC2D, to simulate the upper-covering sand layer shear-band development pace and the scope of a growth normal fault slip. The simulation results indicated an outcome similar to that of the sandbox experiment.

According to the above test results, the Guandu(關渡) profile geometric simulation model established in this study, The PCF2D program was used to create a model for simulating SCF-8 and SCF-9 profiles and the shear-band propagation reached the particle surface in the final 1-m, 2-m, and 2.5-m slip of this growth normal fault numerical model. The simulation results can be applied to the design of construction projects near fault zones.

Keywords: Normal Fault; Shanchiao Fault; Discrete Element Method PFC2D; Transmission Trunks

Sheng-Shin Chu, Professional Fellow, Weatherhead East Asian Institute, Columbia University, 420 West 118th Street, 928, New York, NY 10027; Executive Engineer, Taipei Water Department, 131, ChangXing Street, Taipei 10672, Taiwan, R.O.C.

Chin-Ling Huang, Sub-division Chief, Taipei Water Department, , 131, ChangXing Street, Taipei 10672, Taiwan, R.O.C.

Kai-Ping Chang, Senior Engineer, Engineering Division, Taipei Water Department, 3F., 92, Sec.4, Roosevelt Rd., Taipei 10091, Taiwan, R.O.C.

INTRODUCTION

The National Science and Technology Center for Disaster Reduction (NCDR) of Taiwan has analyzed for large-scale earthquake shocks in the Metropolitan Taipei area. The "Large-scale earthquake impact analysis in the Metropolitan Taipei area" (102- 104) conducted by NCDR for the "disaster impact" and "urban function failure", based on the existing technical deficiencies, the development of relevant assessment techniques to quantify the large-scale seismic shocks in Taipei, as a contingency plan basis and disaster prevention of a large-scale earthquake would hit.

The seismic focal mechanism is considered to be the Shanchiao Fault which is adjacent to the Metropolitan Taipei area. The magnitude of the earthquake is about 7.1, and the depth of the epicenter is about 10 km. The potential of the disability is also estimated. However, the NCDR's estimate of the above-mentioned water and electricity disability has not been conducted for Taipei Water Department (TWD), but TWD should establish its own earthquake-resistant assessment mechanism for the important equipment.

Fractured underground faults form transient and strong seismic waves that are transferred upward and laterally, causing strong ground motion (dynamic behavior) and permanent (or plastic) deformation of the ground surface (static behavior). These two mechanisms can cause severe damage to structures on the ground surface, particularly to those near the fault zone. Although the active reactions of structures induced by transient waves have been thoroughly investigated, ruptures near the ground surface caused by fault fracturing produce permanent or plastic deformation, thus severely distorting and damaging structures and utility pipelines.

As a result of the investigation of the devastating earthquake, it can be seen that the secondary disaster caused by the damage of the major traffic construction and the lifeline near the fault zone is the main cause of the loss of human life and property. The Metropolitan Taipei is the political and economic center of Taiwan, after Pleistocene, northern Taiwan was subject to the clockwise turning and westward extension effect of Okinawa trough, the east-west horizontal tension stress replaced the original compression stress and became the main tectonic stress that influences the crust deformation in northern Taiwan and therefore the thrust faults formed by compression stress during orogeny period has lost their activity mechanism and it is not possible to become active again in recent geologic period. However, according to the distribution map of Taiwan's active fault in 2010 published by the Central Geological Survey of the Ministry of Economic Affairs of Taiwan and a geological survey commissioned by Taiwan Power Company pointed out that this normal fault extends at least 40 km offshore as shown in Figure 1. Shanchiao Fault is a normal fault under the above-mentioned tensile stress in Taipei Basin area, therefore, Shanchiao Fault still remains its activity from the stress point of view.(Lin 2005)

Furthermore, the consequences of fault fractures in proximity to facilities such as reservoirs or nuclear power plants are even more catastrophic and these facilities cannot tolerate differential settlement. Therefore, the key design concept of crucial facilities is to avoid active faults. However, for linear facilities, such as roadways, utility lines, or transmission pipelines, it is impossible to avoid active faults because they must cross them to satisfy transportation and supply needs.

In order to improve the water supply system to New Tamsui residential area and the nearby area, TWD plan and construct a Dadu Transmission Trunks (Dadu line Project) which is a 1200mm water pipeline from the Dadu distribution reservoir to connect the Taiwan Water Company pipeline, and is expected to complete two work wells, a 2000 mm shield tunnel and 1200mm DIP in the shield tunnel, and also with the excavation, the total length of the shield tunnel is about 2,249 m. The construction site is located at the Guandu Plain in the northwestern margin of the Taipei Basin. According to the drilling survey of SCF-7, SCF-8 and SCF-9 conducted by the Central Geological

Survey(CGS) , National Taiwan University's Prof. Chen drew the Guandu section of the Shanchiao fault (as shown in Fig. 2), and determined the position of the fault which is expected to pass the west side of the Dadu Transmission Trunk's 1k + 500 ~ 1k + 600 around. The impact of this activity of the fault has become a very worthy subject.

SURVEY OF RESEARCH REGIONAL TOPOGRAPHY AND GEOLOGY

Dadu line project is located in the Guandu Plain in the northwestern margin of the Taipei Basin. The topography is gentle and the altitude is between 0m-10m. The stratum is dominated by modern alluvial (the Songshan layer of the surface of the Taipei Basin) consist of the nonconsolidation of sand accumulation. Near the end of the pipeline is the Datun volcano area, the formation is mainly the Andesite volcanic breccia.

According to the survey data of the CGS in 2000 and 2010, there are a few faults get through this area, which are Xinzhuang fault, Jinshan fault and Shanchiao fault from the west to the east, and only the Shanchiao fault is the second type active fault, the others are Non-active. The Xinzhuang fault is about 0.2km passed on west of the site, the Shanchiao fault and Jinshan fault pass through the pipeline, and are covered by the Songshan layer of the basin.

Following a single rupture event of a normal fault, the sedimentary layer typically forms from the footing and hanging-wall sides of the normal fault. Because the sedimentary layers in both sides are sufficiently thick to become a single sedimentary layer, the sedimentary layer with the normal fault underneath is thus considered the growth normal fault (Roberts, Yielding et al. 1990). Several rupture events and sediment layers above the normal fault are also possible. Previous studies have indicated that the Shanchiao Fault is a growth normal fault based on drilling and dating information (Huang, Rubin et al. 2007, Chen, Lee et al. 2010). The growth fault sketch map is as shown in Fig.3.

METHODOLOGY

The authors conducted laboratory testing to explore the shear-band propagation in growth normal faults(Chu, Lin et al. 2013). Based on the test results, it is concluded that if there is any seismic activity of a growth normal fault with sandy material, with a smaller offset displacement from the fault tip, although the depositional thickness of the upper layer might be very thick, the shear band could still be propagated to the ground surface as shown in Fig.4.

Moreover, when the fault ruptures, both the rock mass (reverse fault, etc.) or the deposited soil (normal fault) will crack to form the shear zone or the fault zone belt. The strength of soil in this zone (fault gouge) should be weaker than that of general soil. Numerical simulation using continuum if does not consider this phenomenon, the soil strength properties will affect the impact of the simulation results biased the safety side and misjudgment fault rupture caused by future.

In order to properly simulate this phenomenon, the authors collected the literature found that use of discrete element method can do better than a continuum simulation on fault as a good performance of the discrete characteristics of the material. In recent years there have been many studies of fault modeling using this Discrete Element Method (DEM).(Seyferth and Henk 2006, Chang, Lee et al. 2013, Yang, Hu et al. 2014). In this study, the authors established numerical models using the discrete element method, PFC 2D that simulated geological boring profiles SCF-8 and SCF-9 located in the Guandu area, to compare the possible depths of the shear band in the sedimentation layer above the normal fault.

The authors hope that the stress and strain phenomena and distribution of the soil can be observed as the design basis of engineering and disaster mitigation, but the discrete element method can now observe the particle movement and pore change in

the simulation area by using the observing circle or triangular mesh to infer stress changes. However, the application of the aforementioned in soil strain observation of the stimulation area is still inadequate. Because the extent of shear strain could not be shown in the PFC2D program. The shear bands were able to be distinguished by strain ellipse according to the analytical method of structural geology suggested by Ramsay (Ramsay and Huber 1983), using MATLAB software as a postprocessor to translate a grid-history text-data file which was produced through PFC2D simulation. The appropriate number of particles in the models comprised a square area, as shown in Fig. 5, which created a circular area in the center of the square. When the square is affected by single shears, the circle in the center becomes an ellipse, referred to as the finite strain ellipse, as shown in Fig. 6. The finite strain ellipse obtains the value of the shear strain of the original square affected by the shearing effect.

$$R = \frac{a}{b} \quad (1) \quad \Delta_A = \frac{A_{after}}{A_{before}} \quad (2) \quad \frac{a}{r} = R(1 + \Delta_A) \quad (3) \quad \tan 2\theta' = -\frac{2}{\gamma}$$

(4)

where R is the ellipticity; a is the long radius of the finite strain ellipse; b is the short radius of the finite strain ellipse; Δ_A is the volume strain; A_{after} is the area of the original square; A_{before} is the area of the parallel square after shearing; r is the radius of the original circle; θ' is the dip angle of the finite strain ellipse; and γ is the shear strain, as shown in Fig. 6. The ellipticity is the ratios of the long and short axes of the finite strain ellipse. This physical quantity can be used to represent the probe affected by the shearing reaction. The larger the shearing force, the narrower and longer the finite strain ellipse is, and the greater the ellipticity is.

The finite strain ellipse can fully describe the conditions of objects being sheared. The ellipticity, shear strain γ , the dip angle of the finite strain ellipse, volume strain, and the relationships of maximum extension are shown in Table 1. In this study, ellipticity was primarily used to describe the level of reaction when the probe is sheared. Diverse ranges of ellipticity have various color reactions. In this reaction, the ellipticity range of 1.03 (light green color) or above indicated shearing bands.

RESULTS OF THE PFC2D SIMULATION OF GROWTH NORMAL FAULT PROFILES NEAR THE GUANDU AREA

The PCF2D program was used to create a model simulating SCF-8 and SCF-9 Guandu profiles, in which the microscopic coefficients of the numerical model are shown in Table 2. The model involved creating a normal fault by triggering a 1.06 m offset from the fault tip, and allowing a layer of particles to deposit a 0.68-m-thick layer above the footwall and a 1.74-m-thick layer above the hanging wall of the normal fault. A second 1.06 m offset was triggered from the fault tip to create another normal fault offset displacement, allowing another layer of particles to deposit a 0.68-m-thick layer above the footwall and another 1.74-m-thick layer above the hanging wall of the normal fault. The slip and deposition were repeated 205 times so that footwall sediments deposited over 139.4 m and hanging wall sediments deposited over 356.7 m to simulate the SCF-8 and SCF-9 profiles is shown in Fig. 8.

The shear-band propagation of Guandu profiles after slip 1.06m repeatedly 205 times so that footwall sediments deposited over 139.4 m and hanging wall sediments deposited over 356.7 m is shown in Fig. 9.

According to the research of Wells and Coppersmith (Wells and Coppersmith 1994), the normal fault slip induced earthquake magnitude 7.1, the maximum displacement is 2.6m based on empirical estimation as below:

$$\log(\text{MD})=-5.90+0.89*M \quad (5)$$

The shear-band propagation of Guandu profiles after slip 2.0m and 2.5m repeatedly 205 times so that footwall sediments deposited over 139.4 m and hanging wall sediments deposited over 356.7 m is shown in Fig. 10. and Fig. 11.

CONCLUSION AND DISCUSSION

The results of numerically simulating a growth normal fault around Guandu area indicated that with a depositional layer on top of the deformed normal fault, another 1.06m offset event from the normal fault tip can propagate the shear band to the ground surface with a width of 64m. In addition, the distance of the vertical projection from the fault line to the shear band is 69m as shown in Fig.12.

The results of numerically simulating around Guandu area indicated another 2.0m offset event from the normal fault tip can propagate the shear band to the ground surface with a width of 92m. The distance of the vertical projection from the fault line to the shear band is 42m. In addition, 2.0m offset event from the normal fault tip can propagate the shear band to the ground surface with a width of 93m. The distance of the vertical projection from the fault line to the shear band is 41 m.

In a growth normal fault, the offset occurrence from the fault tip causes the shear band to continue from the end of the old shear band to develop upward. This explains why the shear band developed to the ground surface with a smaller offset ratio compared with a regular-normal fault.

The geotechnical and geological survey of the Shanchiao Fault indicated that it remains a highly-active normal fault. Drilling and dating information further proved the existence of a 100 to 700 m thick depositary layer on top of the normal fault, which accumulated after several rupture and deposition events. Although the fault tip might be deeply buried, based on the findings of this study for sandy material, the shear band with a small offset ratio at the growth normal fault tip could develop to the ground surface. Therefore, the ground deformation characteristics near Dadu line that are adjacent to a potential growth normal fault must be considered to avoid any catastrophic failures of the Transmission Trunks.

Table1 Definition of the finite strain ellipse

<i>Finite strain ellipse</i>							
<i>ellipticity</i>	1.0	1.5	2.0	2.5	3.0	3.5	4.0
γ	0%	41%(4%)	71%(7%)	95%(10%)	115%(13%)	133%(16%)	150%(>18%)
θ°	None	-39.2°	-35.2°	-32.3°	-30.0°	-28.1°	-26.6°
<i>Max elongation</i>	1.0	1.5	2.0	2.5	3.0	3.5	4.0
<i>color(砂箱)</i>	1.0~1.5	1.5~2.0	2.0~2.5	2.5~3.0	3.0~3.5	3.5~4.0	4.0~
<i>color(剖面)</i>	1.0~1.03	1.03~1.06	1.06~1.09	1.09~1.12	1.12~1.15	1.15~1.18	1.18~

Table2 The microscopic parameters of the numerical models

Parameters	Values
Ball radius/percentage of weight (m/%)	1.0m/(25%)、0.9 m/(25%)、0.8 m/(25%)、0.7 m/(25%)
Normal stiffness of ball, k_n (N/m)	$k_n = k_{no} \left(\frac{v}{r}\right)^{0.4}$; $k_{no}=4.08 \cdot 10^6$ N/m
Shear stiffness of ball, k_s (N/m)	$1/3k_n$
Normal stiffness of wall	$6.0 \cdot 10^{12}$ N/m
Shear stiffness of wall	$6.0 \cdot 10^{12}$ N/m
Friction coefficient of between ball	0.577 ($\mu = 30^\circ$)
Friction coefficient of between ball and side wall	0.0
Friction coefficient of between ball and base wall	0.364
Density of ball (kg/m^3)	2600

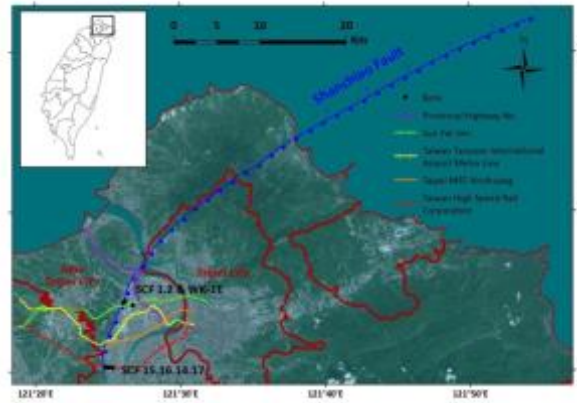


Fig. 1. Trace of Shanchiao Fault.

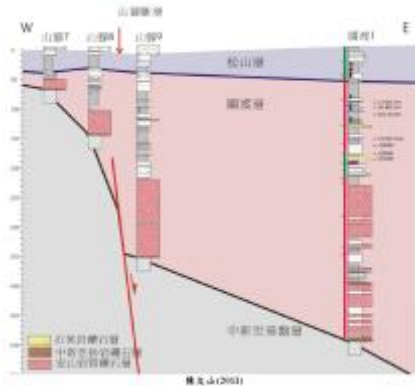


Fig.2. The borehole profile of the SCF-7, SCF-8, and SCF-9 (plotted by Chen, 2011)

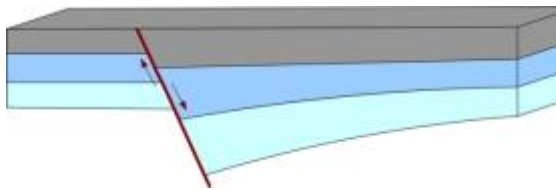


Fig.3. The sketch map of growth fault

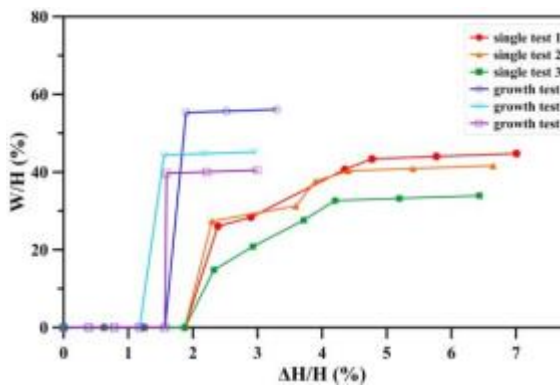


Fig. 4. Relationship of offset ratio ($\Delta H/H$) and normalized influenced width (W/H) for Type 1 (single) and Type 2 (growth) tests.

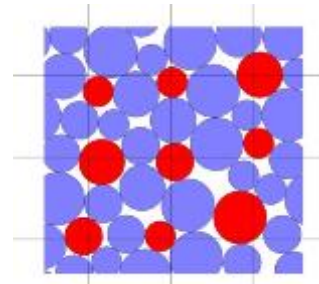


Fig. 5. The finite strain ellipse grid of PFC2D

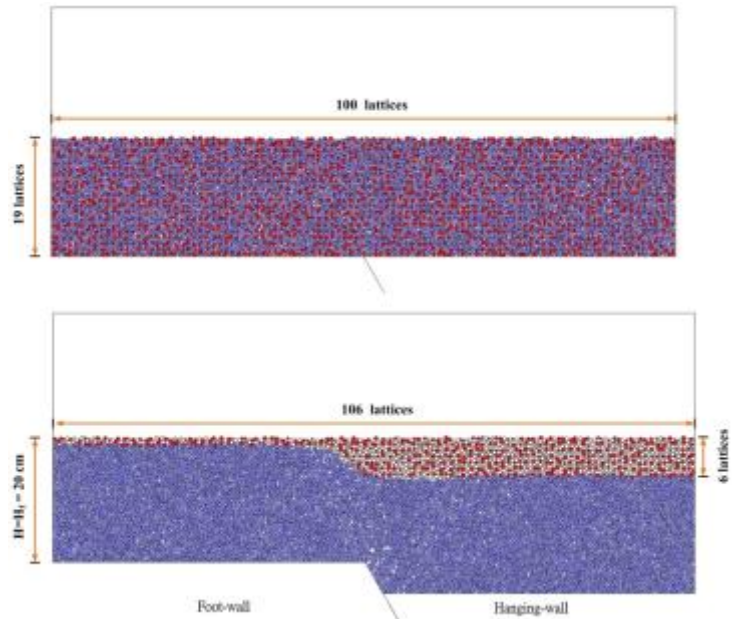


Fig. 6. The finite strain ellipse grid in normal growth fault model of PFC2D

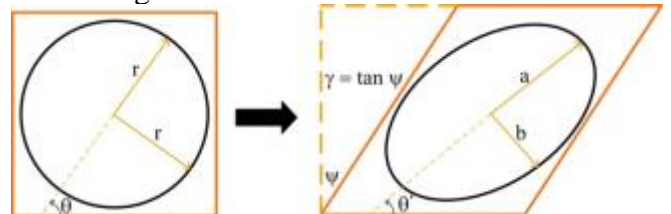


Fig. 7. Using ellipse to describe the shearing reaction of squares (modified from (Ramsay and Huber 1983))

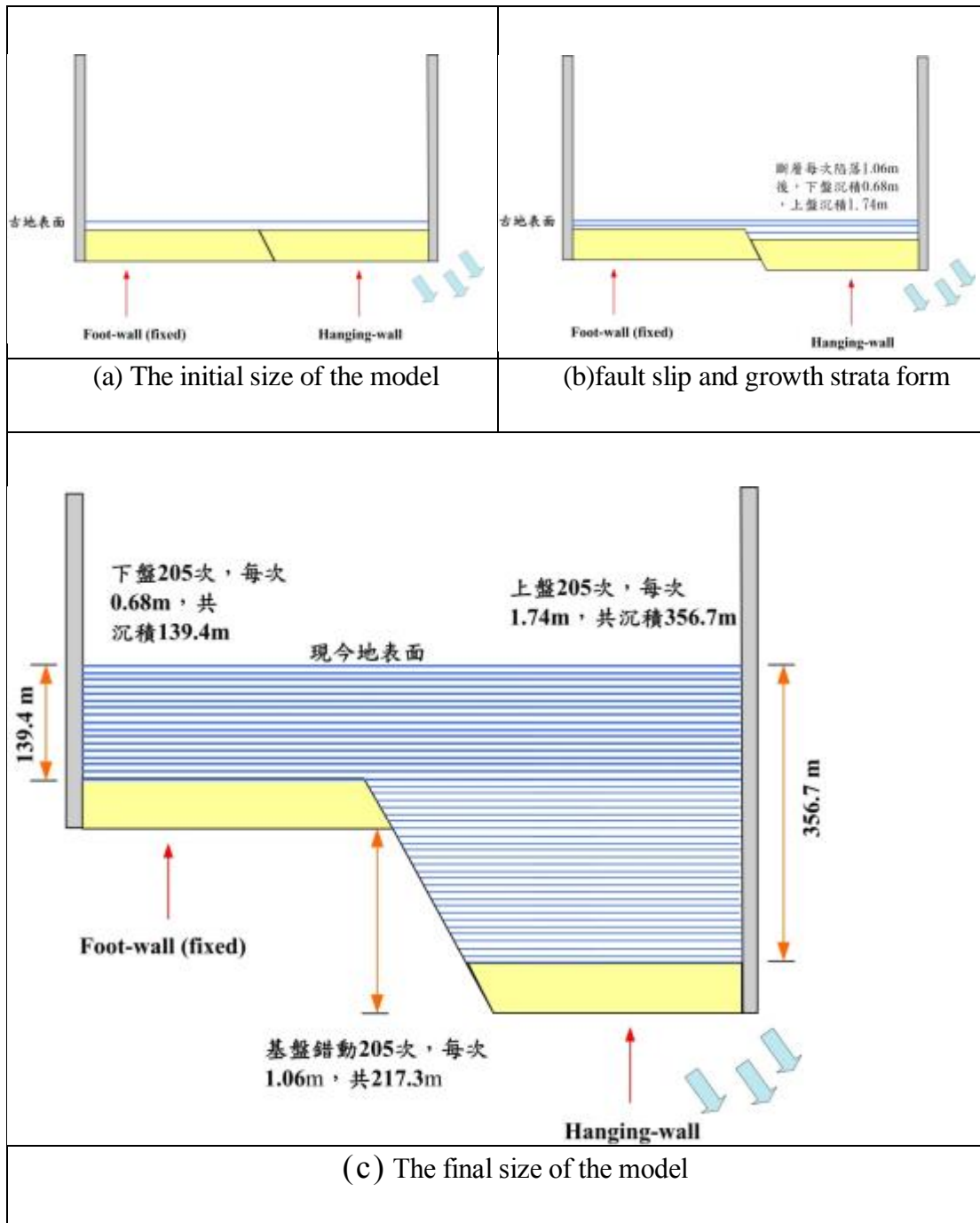


Fig. 8. Guandu profile numerical simulation process and scale illustration

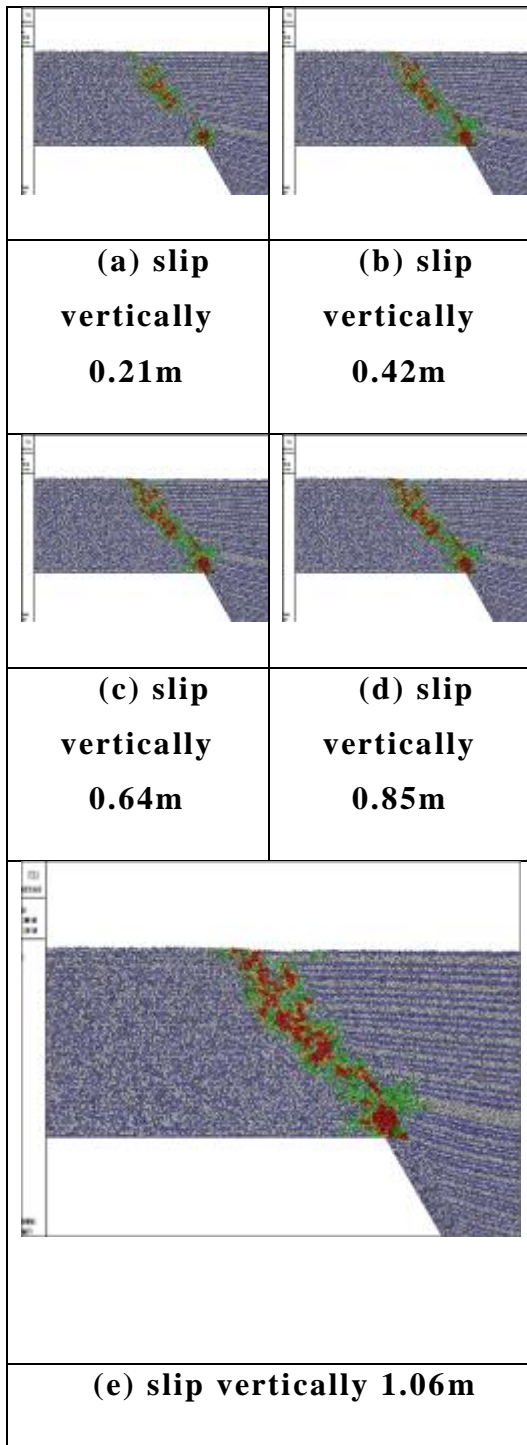


Fig. 9. Process of Guandu profile numerical simulation slip vertically 1.06m

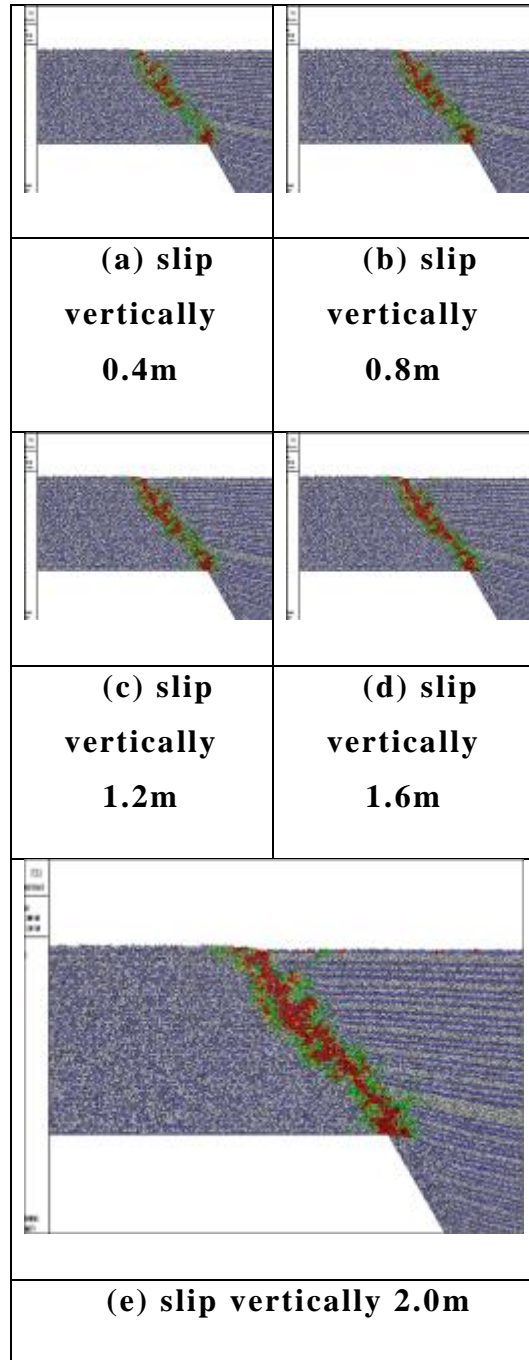


Fig. 10. Process of Guandu profile numerical simulation slip vertically 2.0m

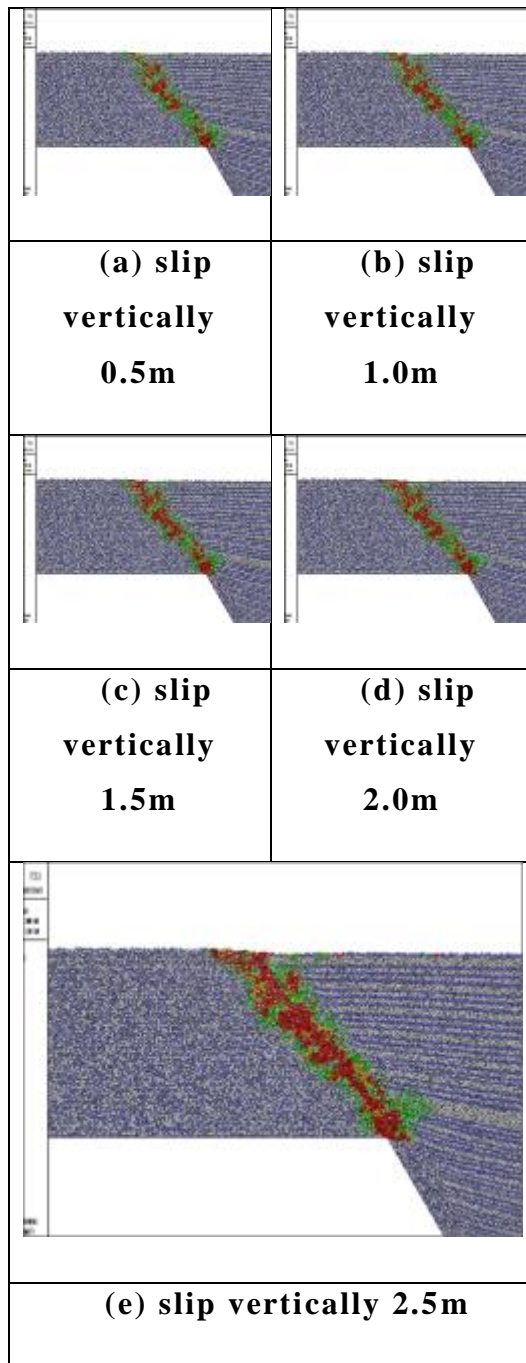


Fig. 11. Process of Guandu profile numerical simulation slip vertically 2.5m

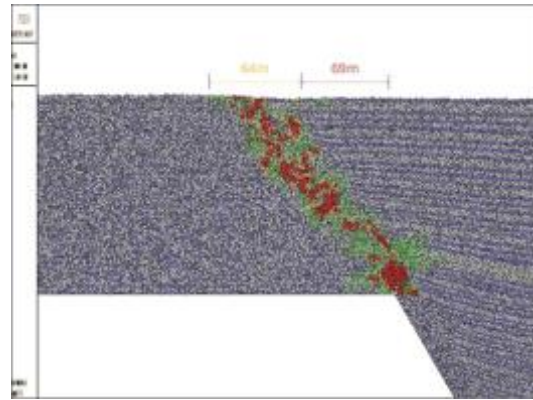


Fig. 12. The shear band propagation by the fault slipped of PFC2D Guandu profile model

REFERENCES

Chang, Y.-Y., C.-J. Lee, W.-C. Huang, W.-J. Huang, M.-L. Lin, W.-Y. Hung and Y.-H. Lin (2013). "Use of centrifuge experiments and discrete element analysis to model the reverse fault slip." International Journal of Civil Engineering **11**(2): 79-89.

Chen, C. T., J. C. Lee, Y. C. Chan and C. Y. Lu (2010). "Growth Normal Faulting at the Western Edge of the Metropolitan Taipei Basin since the Last Glacial Maximum, Northern Taiwan." Terrestrial Atmospheric and Oceanic Sciences **21**(3): 409-428.

Chu, S. S., M. L. Lin, W. C. Huang, H. C. Liu and P. C. Chan (2013). "Laboratory simulation of shear band development in a growth normal fault." Journal of GeoEngineering **8**: 19-26.

Huang, S. Y., C. M. Rubin, Y. G. Chen and H. C. Liu (2007). "Prehistoric earthquakes along the Shanchiao fault, Taipei Basin, northern Taiwan." Journal of Asian Earth Sciences **31**(3): 265-276.

Lin, C. Z. (2005). Shanchiao Fault and Geological Structure of West Edge of Taipei Basin. Symposium on Volcanic Activities and the Shanchiao Fault in the Taipei Metropolis.

Ramsay, J. G. and M. I. Huber (1983). The Techniques of Modern Structural Geology.

Roberts, A., G. Yielding and B. Freeman (1990). "Conference Report - the Geometry of Normal Faults." Journal of the Geological Society **147**: 185-187.

Seyferth, M. and A. Henk (2006). "A numerical sandbox: high-resolution distinct element models of halfgraben formation." International Journal of Earth Sciences **95**(2): 189-203.

Wells, D. L. and K. J. Coppersmith (1994). "New Empirical Relationships among Magnitude, Rupture Length, Rupture Width, Rupture Area, and Surface Displacement." Bulletin of the Seismological Society of America **84**(4): 974-1002.

Yang, Y.-R., J.-C. Hu and M.-L. Lin (2014). "Evolution of coseismic fault-related folds induced by the Chi-Chi earthquake: A case study of the Wufeng site, Central Taiwan by using 2D distinct element modeling." Journal of Asian Earth Sciences **79**, Part A(0): 130-143.